



Bachelor's Thesis

# Fourier transform spectroscopic study of $V_3Al$

conducted at  
Institute of Solid State Physics  
Vienna University of Technology  
Wiedner Hauptstraße 8-10  
1040 Wien

under supervision of  
**Univ.Prof. Dr. Andrei Pimenov**

and

**Evan Constable, PhD**

and

**Dipl.-Ing. Lorenz Bergen**

by

**Maximilian Moser**



# Contents

<b>1</b>	<b>Introduction</b>	<b>5</b>
<b>2</b>	<b>Basics of Fourier transform spectroscopy</b>	<b>6</b>
2.1	Structure and function of the spectrometer . . . . .	6
2.2	Michelson interferometer . . . . .	6
2.3	Fourier transformation . . . . .	7
2.4	Advantages of Fourier transform spectroscopy . . . . .	8
<b>3</b>	<b>Method of Measuring</b>	<b>9</b>
<b>4</b>	<b>The Sample <math>V_3Al</math></b>	<b>11</b>
4.1	Theory . . . . .	11
4.2	Spectra in ambient temperature . . . . .	11
4.3	Measuring under magnetic field . . . . .	14
<b>5</b>	<b>Cooling <math>V_3Al</math></b>	<b>17</b>
<b>6</b>	<b>Summary and Outlook</b>	<b>18</b>



# 1 Introduction

The task of this Bachelor's Thesis was to conduct measurements on  $V_3Al$  under both room temperature and low temperature up to 10 K.  $V_3Al$  has been described theoretically by *Jamer et al.* in [1]. A goal in this thesis was to measure some of the electronic properties described in this paper. These properties are explained in subsection 4.1 on page 11. Additionally a custom sample holder was constructed to measure any electronic properties under low magnetic field at room temperature.

In the beginning of this thesis, a brief overview of the basics of Fourier transform spectroscopy, the measuring technique used in all conducted experiments, is given. Afterwards the experimental setup and methods of measuring is explained. Then the theory on  $V_3Al$  is explained and the experimental results are shown. In the end, a short summary of the most important experimental results is given.

## 2 Basics of Fourier transform spectroscopy

### 2.1 Structure and function of the spectrometer

Fourier transform spectroscopy uses the interference between two beams of electromagnetic radiation with a path difference to produce an interferogram. This signal is measured as a function of the change in path difference between the two beams. The interferogram is then converted into a spectrum via Fourier transformation [2, page 18-19].

### 2.2 Michelson interferometer

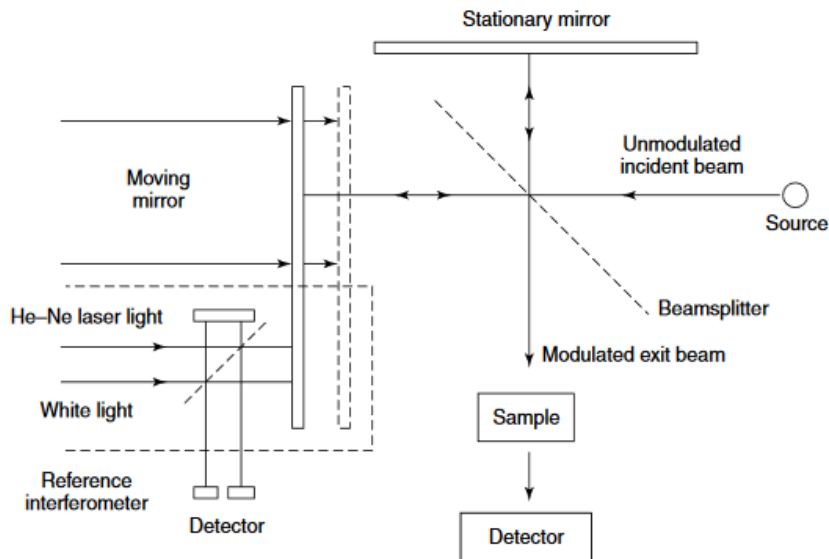


Figure 1: Schematics of a Fourier transform spectrometer [2, page 19].

Typically, a Fourier transform spectrometer functions using a Michelson interferometer. This consists of two plane mirrors, one of which can be moved perpendicular to its plane and a beam splitter, that is chosen depending on the region of wavelength to be examined. By moving the mirror a path difference is created. This leads to constructive and destructive interference that can be seen in Figure 2. A systematic figure of the structure of a Fourier transform spectrometer with a Michelson interferometer is shown in Figure 1. The small interferometer shown in Figure 1 in the lower-left corner is used to measure the exact position of the moving mirror [2, page 18].

## 2.3 Fourier transformation

Only one formula is needed to perform a Fourier transformation of the interferogram to obtain the intensity  $I$  as a variation of the wavenumber  $\bar{\nu}$ :

$$I(\bar{\nu}) = \int_{-\infty}^{+\infty} \hat{I}(\delta) \cdot \cos(2\pi\bar{\nu}\delta) d\delta. \quad (1)$$

Here  $\delta$  is the difference in the beam path and  $\hat{I}$  the measured intensity of the interferogram.

The following formula could be used to reverse this process:

$$\hat{I}(\delta) = \int_0^{+\infty} I(\bar{\nu}) \cdot \cos(2\pi\bar{\nu}\delta) d\bar{\nu}. \quad (2)$$

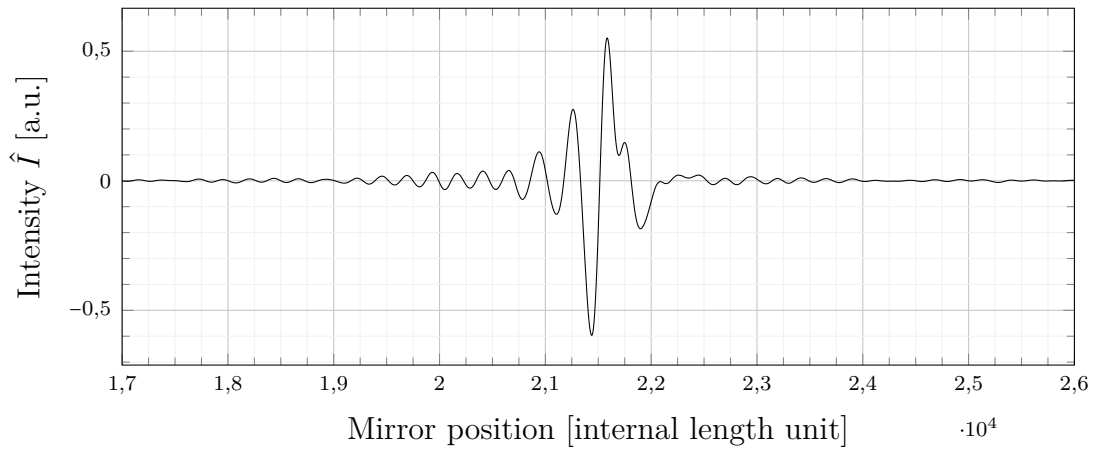


Figure 2: Interferogram of the gold mirror reference.

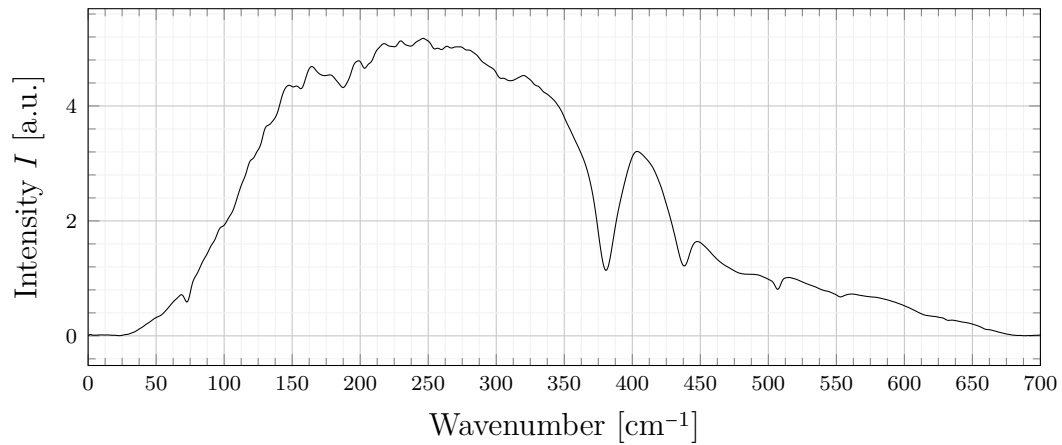


Figure 3: Frequency spectrum, obtained by a Fourier transform of the interferogram (Figure 2).

## 2.4 Advantages of Fourier transform spectroscopy

One of the main advantages of Fourier transform spectroscopy is the fast scan time. This leads to lowering the signal-to-noise ratio by averaging the signal over all of its scans. In addition because slits or other restricting devices such as gratings are not used, a relatively high radiation flux can be directed onto the sample. So a higher signal is recorded at the detector, which also lowers the noise [2, page 23].

### 3 Method of Measuring

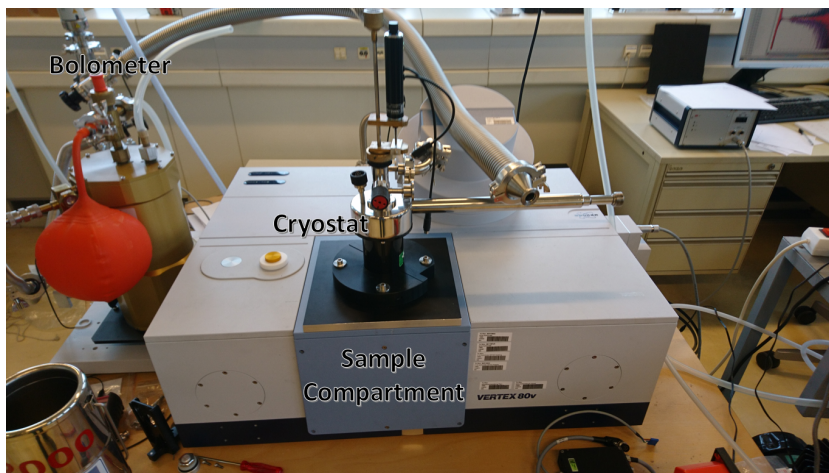


Figure 4: Photograph of *Bruker* VERTEX 80v.

The spectrometer used in this project was a *Bruker* VERTEX 80v (see Figure 4). It consists of a vacuum chamber with the infrared (IR) sources, the Michelson interferometer, a sample compartment for the sample and the gold reference, as well as various detectors optimised for different spectral bandwidths. Additionally the far infrared bolometer detector is mounted outside of the chamber. The sample compartment can be vented independently to assist in faster sample changes. The basis arrangement of the optical elements agrees with Figure 2. In Figure 5 the real beam path of the spectrometer is shown. The vacuum (around 2 hPa) is used to minimize the absorption from water molecules in the air.

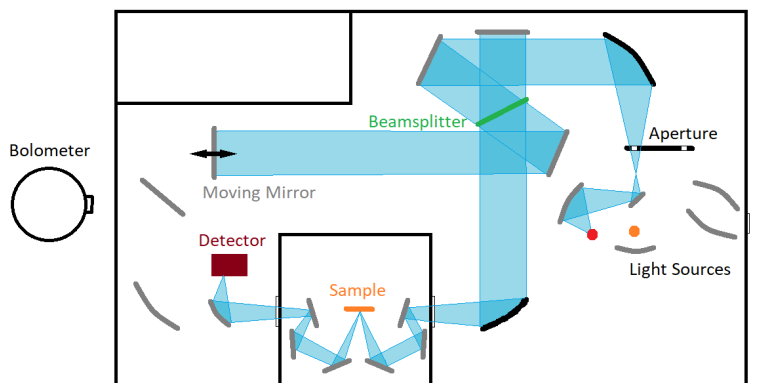


Figure 5: Beam path of the VERTEX 80v from *Bruker*.

This setup is designed to work over a broad spectral range. Since most of the optical

parts are working only in a certain optical frequency range it is necessary to use different optical elements to cover the entire spectral range. An overview is given in Table 1.

Setting	Spectral Range [ $\text{cm}^{-1}$ ]	Source	Beamsplitter	Detector
NIR	25000 - 8000	Tungsten Lamp	$\text{CaF}_2$	Silicon Diode
NMIR	12000 - 3000	Tungsten Lamp	$\text{CaF}_2$	MCT
MIR	5000 - 500	Glowbar	KBr	MCT
FIR	680 - 30	Mercury Lamp	Mylar 6 $\mu\text{m}$	Bolometer
THz	60 - 10	Mercury Lamp	Mylar 50 $\mu\text{m}$	Bolometer

Table 1: Table of measuring ranges (near infrared NIR, near-mid infrared NMIR, mid infrared MIR, far infrared FIR).

To obtain a reflectivity spectrum of a sample, both the interferograms of the sample and of a gold reference must be measured under the same conditions (number of scans, aperture, etc.). Then these are Fourier transformed by the computer and the corresponding spectrum of the sample is divided by the reference spectrum. This quotient is the reflectivity. The Fourier transformation is done with the software OPUS by *Bruker*.

Usually a gold mirror is used as the reference because of its almost perfect reflectivity over a broad spectral range [3].

## 4 The Sample $V_3Al$

### 4.1 Theory

$V_3Al$  is a spin gapless semiconductor (SGS) [4]. Those materials have spin-polarized carriers as well as novel semiconducting properties [5]. Figure 6 shows an illustration of the band gap of  $V_3Al$ . Here we find that for one spin type the system behaves like a metal with a gapless band structure. For the other spin type there is a band gap with the fermi level lying between the valence and conduction bands as in a semiconductor.  $V_3Al$  may therefore exhibit interesting spin dependent properties. After *Jamer et al.* [1]  $V_3Al$  is a so called pseudo Heusler compound. These compounds exhibit properties relevant to applications in spintronics, for example variations of the Hall effect, magnetoresistance, ferro-, antiferro-, and ferrimagnetism, emiconductivity with spin filter ability, superconductivity and topological insulation [6].

An effective probe of these properties is to measure the optical conductivity by the reflection of radiation incident on the sample surface. For example a measurement of the spin gap may appear as a step in the reflectivity at a specific frequency equivalent to the energy gap [7]. Magneto resistance may be observed by detecting a change in the optical conductivity under the application of a magnetic field or at lower sample temperatures.

The reviewed sample is a cuboid with a square base with 3x3 mm and a thickness of 1 mm. Both sides are polished to increase the reflectivity.

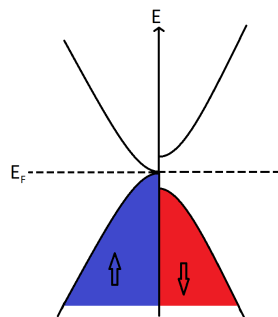


Figure 6: Illustration of the band gap of  $V_3Al$ .

### 4.2 Spectra in ambient temperature

The following spectra were measured under ambient temperature ( $\sim 300$  K). The broadband spectra in Figure 7 and Figure 8 were combined together from the settings listed in

Table 1 in the overlapping areas. The following graphs show a higher reflectivity than 1 in some areas. This could be caused by dust or small scratches on the reference gold mirror. This indicates that more light is being reflected from the sample than the gold reference at these frequencies. This shows that the reference is an imperfect reflector possibly due to surface imperfections. Nevertheless the general trend of the sample reflectivity can be seen to decrease almost linearly.

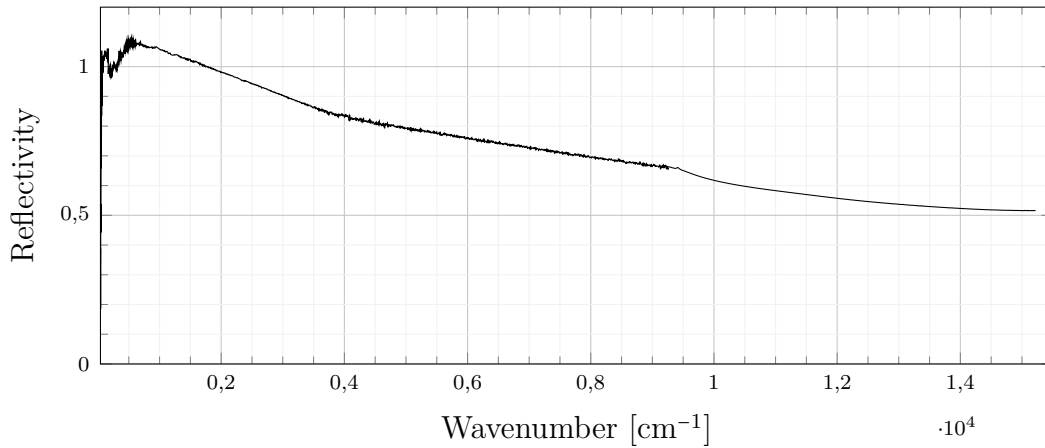


Figure 7: Broadband spectrum of  $V_3Al$ .

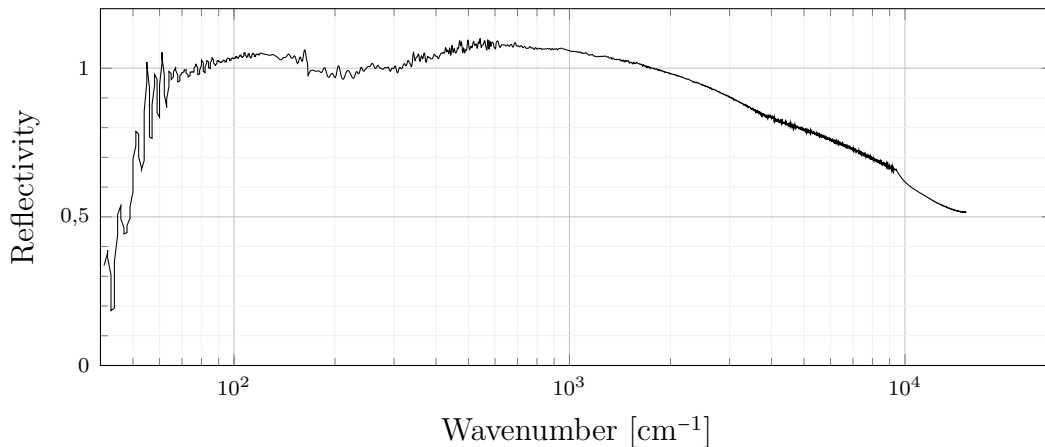


Figure 8: Broadband spectrum of  $V_3Al$  with logarithmic axis.

The high reflectivity (optical conductivity) at lower frequencies is typical of metallic properties.

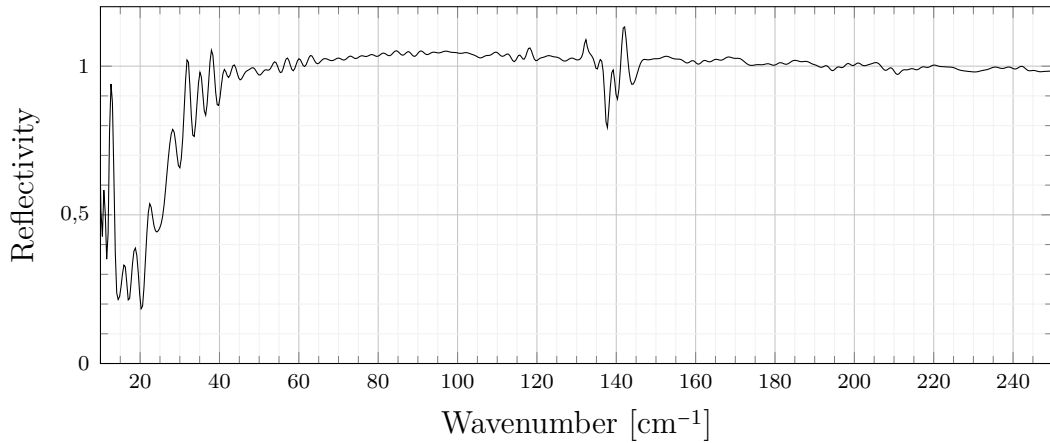


Figure 9: Reflectivity over THz band.

In Figure 9 (THz region) you can see a clear dip in reflectivity between 10 and 30  $\text{cm}^{-1}$ . It is possible that this dip represents the energy of the band gap, however we find that it is likely the result of an artefact due to the small sample and the even smaller hole of the sample holder, because the wavelength of the photons is in the range of the hole of the sample holder. The diameter of the sandpaper mask was around 1.5 mm. 1.5 mm aperture means wave lengths on the order of 1 mm ( $10 \text{ cm}^{-1}$ ) will be diffracted and not contribute to the reflectivity. This means that a part of the incoming light is being absorbed by the sample holder. The spectrum for the gold mirror was acquired with the same aperture, but with a larger reflective surface. The oscillations around  $140 \text{ cm}^{-1}$  are due to a beam splitter minimum.

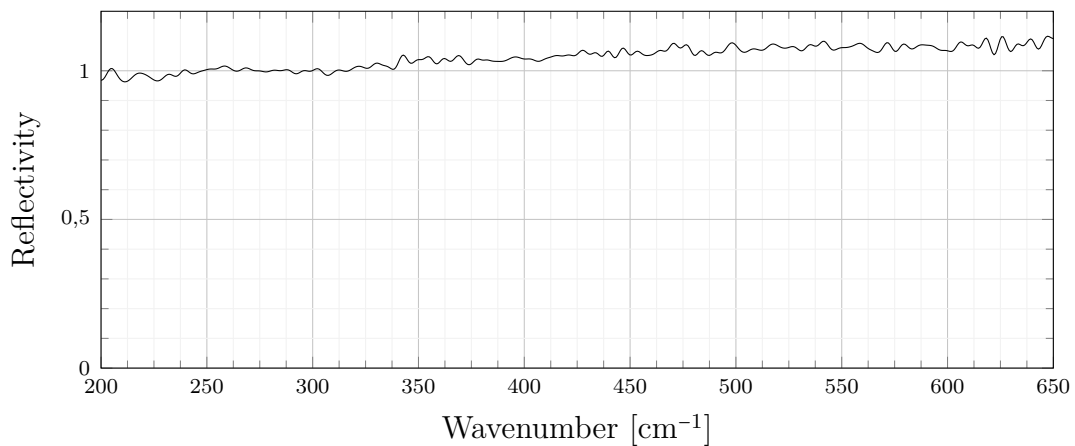


Figure 10: Reflectivity over FIR band.

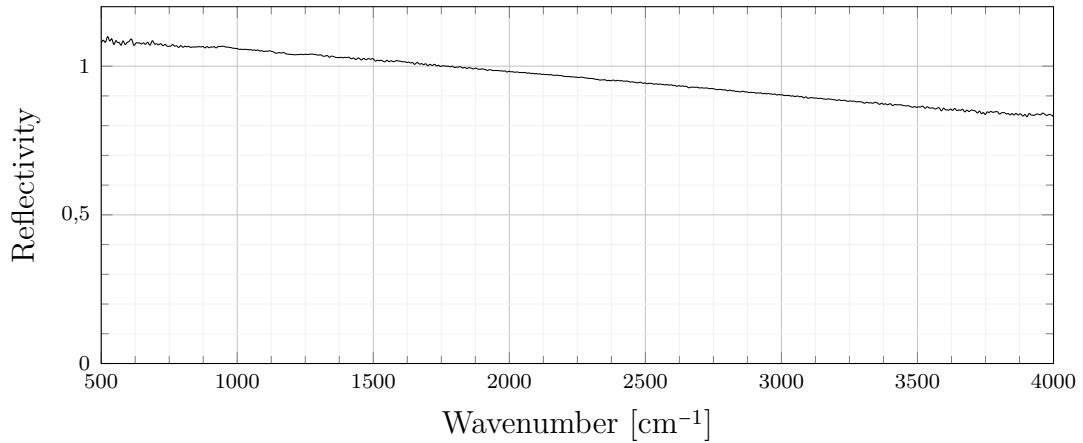


Figure 11: Reflectivity over MIR band.

In Figures 7 to 11 it is clearly visible, that  $V_3Al$  has no significant peaks in the measured range that may have been expected in subsection 4.1. The absence of any optical phonon modes which would be expected in a diatomic alloy such as  $V_3Al$  is likely the result of screening electrons due to the metallic properties. To observe any magnetic dependence on conductivity, reflectivity under magnetic field is measured.

### 4.3 Measuring under magnetic field

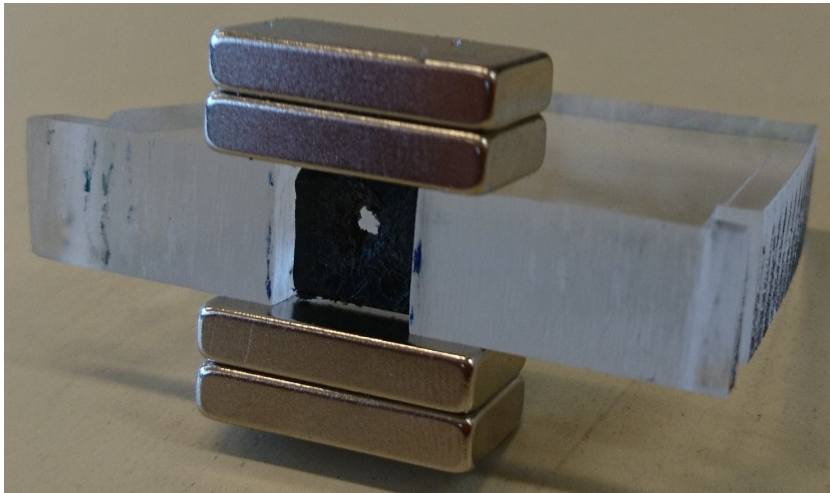


Figure 12: Sample-holder for measuring under magnetic field

For measuring  $V_3Al$  under magnetic field a custom sample-holder, that can be seen in Figure 12 and in Figure 13 has been constructed. Its base material is 1 cm thick

acrylic glass. An indentation was made to allow for the sample to be mounted between the magnets. The magnets are placed on both sides of the acrylic glass and held together tight due to the magnetic forces. Preliminary scans had been performed with different numbers of magnets (between 1 and 2 on each side).

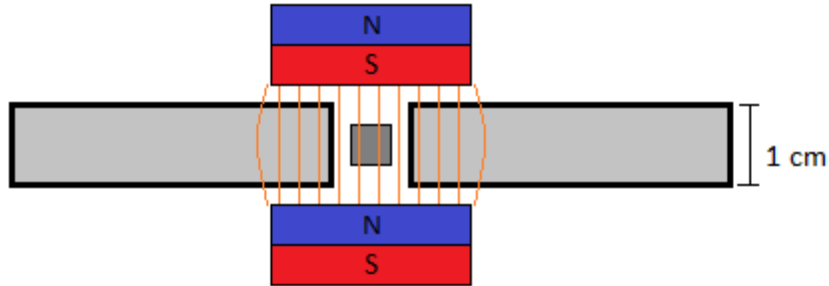


Figure 13: Schematic sketch of sample-holder for measuring under weak magnetic fields.

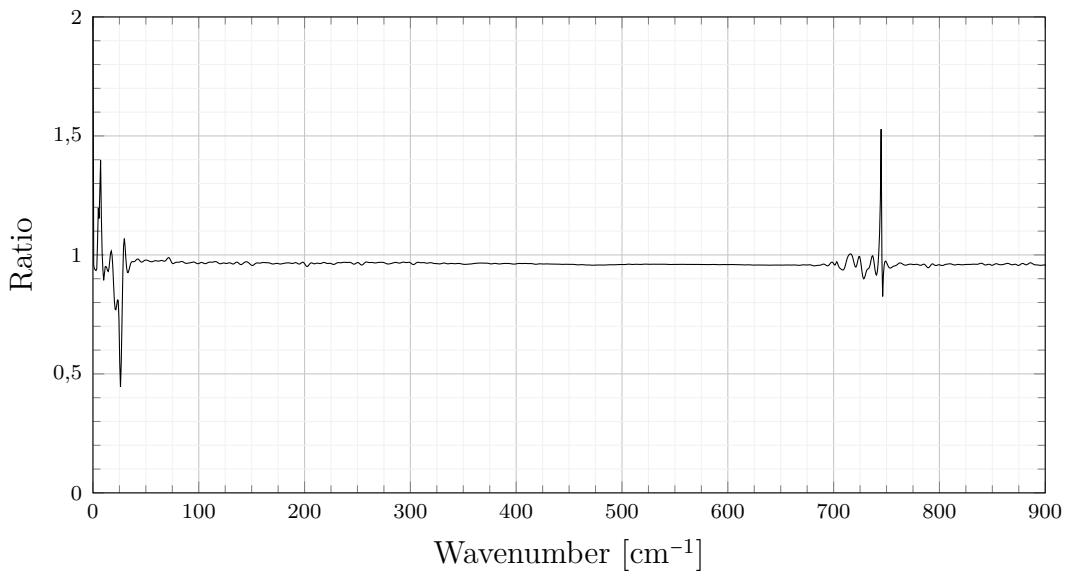


Figure 14: Ratio of reflected intensity between magnetic field and no magnetic field of  $V_3Al$  without polarisation.

In Figure 14 the ratio between magnetic field and no magnetic field of  $V_3Al$  without polarisation is shown. You can clearly see that it is slightly lower than one. This could be due to a reduction in reflectivity under magnetic field, or, more likely, due to slight misalignment while removing the magnets from the sample holder. This is supported by the offset being linear across the whole measured range. The noise at around  $740\text{ cm}^{-1}$  was caused by a beam splitter minimum.

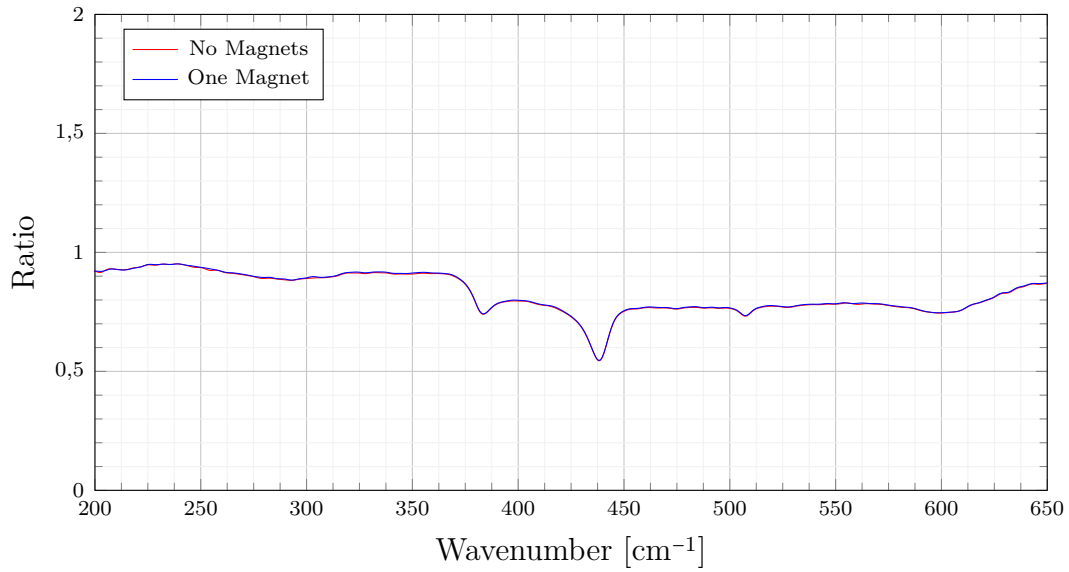


Figure 15: Comparison between the ratio of  $0^\circ$  polarisation and  $90^\circ$  polarisation with and without magnetic field.

The ratio portrayed in Figure 15 is the ratio of  $0^\circ$  polarisation and  $90^\circ$  polarisation with and without magnetic field. As it is clearly seen, those two graphs are almost identical. This means, that there is no change in reflectivity for any direction of polarisation in the measured range, otherwise there would be a difference between the red and the blue graph.

Unfortunately it was not possible to observe any systematic changes in reflection, as seen in Figures 14 and 15. Reasons for this could be, that the measurements were conducted under ambient temperature, or that the magnetic field was too low.

## 5 Cooling $V_3Al$

For cooling the  $V_3Al$  sample a Helium-flow cryostat, produced by *Oxford-Instruments* was used. To cool down the sample and the reference mirror, a constant flow of liquid Helium cools a copper block, which is thermally coupled with the sample and the mirror. A picture of the cryostat mounted in the spectrometer can be seen in Figure 4 on page 9. The typical base temperature lies between 10 and 15 K.

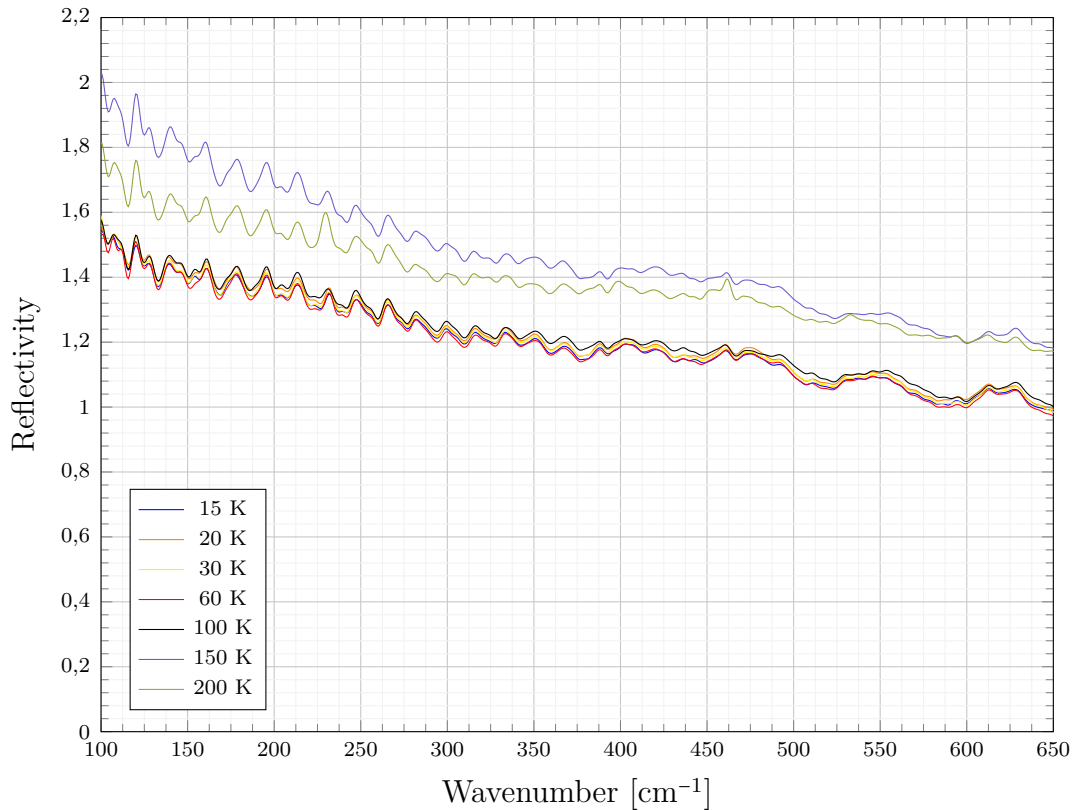


Figure 16: Cooling of  $V_3Al$ .

In Figure 16 you can clearly see, that there are apparent changes in the spectrum with change of temperature, but they are in fact all artefacts. The reflectivity in this graph is higher than one because the sandpaper, that was used to reduce the reflection of the sample holder, slightly covered the gold mirror. The graph for reflectivity for 150 and 200 K is even higher, due to even more misalignment of the sandpaper. The fringes may have been caused by dust or ice on the cryostat windows, but most likely internal reflections of the cryostat windows.

## 6 Summary and Outlook

The reflectivity of a polished  $V_3Al$  sample was measured with a Fourier transform spectrometer under different spectral ranges, from 10 to 10 000  $\text{cm}^{-1}$ , although under 40  $\text{cm}^{-1}$  the signal was not sufficiently good enough. In the far-infrared (FIR) setting measurements were performed additionally under magnetic field and at low temperatures ( $\sim 15$  K) using a Helium-flow cryostat.

Overall the spectra reveal a typical metallic response with no clear changes at low temperature or under weak magnetic fields. So it was not possible to observe any of the effects that were predicted by Jamer (see subsection 4.1). This may be caused by a too weak magnetic field which is also only usable under room temperature conditions.

So for further measurements it would be interesting to measure the sample under higher magnetic field with polarisation at low temperatures. Unfortunately this is not possible due to the used experimental set up, without larger modifications of the cryostat. Additionally it is not clear that the magnetic fields created by the used permanent magnets are large enough to lead to any effects in the sample. The magnitude of the field is even unknown. So as mentioned before higher fields are probably necessary. This would have to be realized with a different source of magnetic field, for example superconducting coils. But these are in fact impossible to use in the existing cryostat.

## References

- [1] M. E. Jamer, B. A. Assaf, G. E. Sterbinsky, D. Arena, L. H. Lewis, A. A. Saúl, G. Radtke, and D. Heiman, “Antiferromagnetic phase of the gapless semiconductor  $V_3Al$ ,” *Phys. Rev. B*, vol. 91, p. 094409, Mar 2015. [Online]. Available: <https://link.aps.org/doi/10.1103/PhysRevB.91.094409>
- [2] B. Stuart, *Infrared Spectroscopy: Fundamentals and Applications*, 2004.
- [3] R. Schiwon, G. Schwaab, E. Bründermann, and M. Havenith, “Far-infrared multilayer mirrors,” *Applied Physics Letters*, vol. 83, no. 20, pp. 4119–4121, 2003. [Online]. Available: <https://doi.org/10.1063/1.1627479>
- [4] X. L. Wang, “Proposal for a new class of materials: Spin gapless semiconductors,” *Phys. Rev. Lett.*, vol. 100, p. 156404, Apr 2008. [Online]. Available: <https://link.aps.org/doi/10.1103/PhysRevLett.100.156404>
- [5] S. Ouardi, G. H. Fecher, C. Felser, and J. Kübler, “Realization of spin gapless semiconductors: The heusler compound  $Mn_2CoAl$ ,” *Phys. Rev. Lett.*, vol. 110, p. 100401, Mar 2013. [Online]. Available: <https://link.aps.org/doi/10.1103/PhysRevLett.110.100401>
- [6] Wikipedia. (03.01.2018) Heusler compound. [Online]. Available: [https://en.wikipedia.org/wiki/Heusler\\_compound](https://en.wikipedia.org/wiki/Heusler_compound)
- [7] F. P. Mena, J. F. DiTusa, D. van der Marel, G. Aeppli, D. P. Young, A. Damascelli, and J. A. Mydosh, “Suppressed reflectivity due to spin-controlled localization in a magnetic semiconductor,” *Phys. Rev. B*, vol. 73, p. 085205, Feb 2006. [Online]. Available: <https://link.aps.org/doi/10.1103/PhysRevB.73.085205>